British Journal of Pharmacology (2007) 152, 132–140

www.brjpharmacol.org

RESEARCH PAPER

A functional comparison of recombinant and native somatostatin sst_2 receptor variants in epithelia

ND Holliday[1], IR Tough and HM Cox

Wolfson Centre for Age-Related Diseases, King's College London, Hodgkin Building, Guy's Campus, London, UK

Background and purpose. Somatostatin (SRIF-14) exerts broad spectrum antisecretory effects by activating the somatostatin 2 (sst_2) receptor. The rat (r) sst_2 receptor exists in 'long' (sst_{2a}) and 'short' (sst_{2b}) forms that differ in their C termini, while a single human (h) sst_{2a} exists. This study compares the characteristics of recombinant $rsst_{2a}$, $rsst_{2b}$ and $hsst_{2a}$ activation in human epithelia, and with native sst_2 responses in rat colon.
Experimental approach. Epithelial layers of each clone or rat colon were placed in Ussing chambers and short-circuit current (I_{SC}) measured in response to SRIF-14 and chosen analogues. The relative potencies and ability to cause desensitization to SRIF-14 were assessed, and the affinities of the sst_2 antagonist, D-Tyr[8] CYN154806 for $hsst_{2a}$, $rsst_{2a}$ and native rat colon sst_2 receptors were established.
Key results. Basolateral SRIF-14 responses were transient in $hsst_{2a}$ and $rsst_{2a}$ epithelia, but prolonged in $rsst_{2b}$-expressing cells. Activation of $rsst_{2a}$ resulted in significant desensitization to SRIF-14 and receptor phosphorylation, whereas the $rsst_{2b}$ receptor did neither. Sst_2-preferred agonists (BIM23190C and BIM23027) reduced I_{sc} with similar potency and both caused complete desensitization to SRIF-14. CYN154806 antagonized $hsst_{2a}$ and $rsst_{2a}$ receptors with pK_B values of 7.9 and 7.8, respectively. In rat colon mucosa, CYN154806 blocked SRIF-14 responses with a pA_2 value of 8.2, and BIM23190C responses with a pK_B of 8.4.
Conclusions and implications. SRIF-14 caused rapid $rsst_{2a}$ receptor phosphorylation and desensitization of epithelial antisecretory responses, neither of which occurred with the $rsst_{2b}$ receptor. These mechanisms are most likely to be a prerequisite for sensitivity to sst_2-analogues with radiotherapeutic potential.
British Journal of Pharmacology (2007) **152,** 132–140; doi:10.1038/sj.bjp.0707365; published online 2 July 2007

Keywords: somatostatin 2 receptor variants; sst_{2a}; sst_{2b}; epithelial ion transport

Abbreviations: D-Tyr[8] CYN154806, Ac-(4-NO_2-Phe)-*cyc*(DCys-Tyr-DTrp-Lys-Thr-Cys)-DTyr-NH_2; DMEM, Dulbecco's modified Eagle's medium; HA, haemagglutinin; hS2a, human sst_{2a} clone; rS2a, rat sst_{2a} clone; rS2b, rat sst_{2b} clone; I_{SC}, short-circuit current; KH, Kreb's Henseleit; SRIF-14, somatotrophin release inhibiting factor (somatostatin)14–28; TTX, tetrodotoxin; VIP, vasoactive intestinal polypeptide; UK14,304, 5-bromo-*N*-(4,5-dihydro-1H-imidazol-2-yl)-6-quinoxalinamine

Introduction

SRIF-14 (somatotrophin release inhibiting factor, or somatostatin-14) is an enteric neuropeptide (Schultzberg *et al*., 1980; Ekblad *et al*., 1988) and endocrine cell product (Alumets *et al*., 1977) with broad spectrum antisecretory effects that include inhibition of gastric acid (Lloyd *et al*., 1995), intestinal electrolytes (Eklund *et al*., 1988; Knobloch *et al*., 1989; Ferrar *et al*., 1990) and endocrine secretions, for example, growth hormone, glucagon and insulin (for a review, see Weckbecker *et al*., 2003). These inhibitory actions are mediated by somatostatin 2 (sst_2) receptors, one of five cloned sst receptor types that couple to pertussis toxin-sensitive $G_{i/o}$ proteins and reduce adenylate cyclase activity (Siehler and Hoyer, 1999b) and can also modulate ion channels, for example, opening neuronal K^+ channels (Hicks *et al*., 1998) or closing voltage-dependent Ca^{2+} channels (Kleuss *et al*., 1991) thereby reducing neuron excitability.

Two sst_2 receptor spice variants are produced in mouse (Vanetti *et al*., 1993) and rat (r) tissues, alternative splicing occurring via a cryptic splice site within the coding sequence of the sst_2 receptor gene (Schindler *et al*., 1998). Both rodent species express an sst_{2a} receptor variant that is 23 amino acids longer than sst_{2b}, but with different C termini (for a review, see Cole and Schindler, 2000). Activation of the murine (m) short isoform, $msst_{2b}$, inhibited adenylate cyclase with greater efficacy and resulted in significantly less agonist-induced desensitization than the $msst_{2a}$ receptor (Vanetti *et al*., 1993). In contrast, no differences were observed between $rsst_{2a}$ and $rsst_{2b}$ signalling or desensitiza-

Correspondence: Professor HM Cox, Wolfson CARD, King's College London, Hodgkin Building, Guy's Campus, London SE1 1UL, UK.
E-mail: helen.cox@kcl.ac.uk
[1]Current address: Institute of Cell Signalling, School of Biomedical Sciences, Floor C, Queen's Medical Centre, Nottingham, NG7 2UH, UK.
Received 15 March 2007; revised 22 May 2007; accepted 1 June 2007; published online 2 July 2007

tion after exposure to SRIF-14 (Schindler *et al.*, 1998). The clearest discrimination between these two receptors' signalling capacities was described for the opposing actions of SRIF-14 on CHO cell proliferation; $rsst_{2a}$-expressing cells exhibiting an inhibition, and $rsst_{2b}$ cells, a stimulation of peptide-induced proliferation (Alderton *et al.*, 1998). In contrast with the proven production of two different sst_2 isoforms in rat and mouse, only the human (h) sst_{2a} has been identified as a functional protein, the $hsst_{2b}$ orthologue remaining putative (see Cole and Schindler, 2000).

The distribution patterns of the two sst_2 variants differ in mouse and rat nervous systems, sst_{2a} predominating in the central and peripheral nervous systems (Sarret *et al.*, 1998; Cole and Schindler, 2000; Schulz *et al.*, 2000). In the gastrointestinal tract, differences are also observed. In rat stomach and small intestine, for example, the sst_{2a} receptor protein is expressed by neuroendocrine cells and enteric nerves (implicating indirect, as well as direct mechanisms of SRIF-14 action), while sst_{2b} receptor labelling is found in a discrete subpopulation of rat parietal cells (Schindler and Humphrey, 1999). Warhurst *et al.* (1996) observed both sst_2 receptor transcripts in rat colonic crypt extracts and with equal abundance. In the mouse stomach, parietal and endocrine cells express sst_2 receptors, as do subpopulations of myenteric and submucous neurons, immunostaining for sst_{2a} being colocalized with nitric oxide synthase immunoreactivity in inhibitory myenteric motor neurons (Allen *et al.*, 2002). In the human gastrointestinal tract, sst_{2a} is also expressed by endocrine cells (particularly, gastrin-containing cells in the small intestine), as well as myenteric and submucous neurons along the length of the intestine (Gugger *et al.*, 2004) and this pattern is similar to that reported in the rat gastrointestinal tract (Schindler and Humphrey, 1999).

The extensive inhibitory nature of SRIF-14 actions stimulated early interest in the peptide for therapeutic benefit, for example, as a novel treatment for diabetes, of hormone-secreting tumours and hypersecretory diarrhoea, but the relative instability of plasma SRIF-14 was limiting. One of the first longer-acting cyclic SRIF-14 fragment analogues, octreotide (SMS 201-995, Sandostatin) is used, for example, to treat acromegaly, to prevent complications following pancreatic surgery and relieve symptoms such as chemotherapy-induced diarrhoea (Lamberts *et al.*, 1996). Many other more stable cyclo-octapeptide analogues have since been produced with therapeutic, as well as diagnostic potential (Weckbecker *et al.*, 2003) and some of these have been used in the present study, specifically, BIM23027 (amino acid sequence is as listed in McKeen *et al.* (1995)), BIM23190C, BIM23014C (Lanreotide) and BIM23268, together with the linear analogues BIM23052 and BIM23056 (amino acid sequences are as listed in Shimon *et al.* (1997)). Sst receptor-mediated endocytosis has also been utilized clinically to deliver stable radiolabelled SRIF-14 analogues into tumour cells that express sst_2 receptors, thereby allowing metastases to be imaged (Breeman *et al.*, 2001) and treated by receptor-targeted radiotherapy (Weckbecker *et al.*, 2003).

The present study set out to determine whether SRIF-14 activation of recombinant $hsst_{2a}$, $rsst_{2a}$ and $rsst_{2b}$ expressed in epithelial cells, differed (i) in their response time courses and pharmacology, (ii) in their agonist-induced phosphorylation and desensitization and (iii) whether their pharmacologies differed from that of native sst_2 antisecretory responses in rat colon mucosa. Two SRIF-14 analogues were chosen for their sst_2 affinity, namely, BIM23190C and BIM23027 (McKeen *et al.*, 1995; Shimon *et al.*, 1997; Siehler *et al.*, 1999; Weckbecker *et al.*, 2003). Also included were other SRIF-14 analogues known to stimulate sst_5 receptors (BIM23268 and BIM23052, Shimon *et al.*, 1997; Weckbecker *et al.*, 2003) and the nonselective $sst_5/sst_2/sst_3$ analogue, BIM23056 (Shimon *et al.*, 1997; Siehler and Hoyer, 1999a,b; Weckbecker *et al.*, 2003) shown also to be an sst_5 antagonist (Wilkinson *et al.*, 1996). The affinity of the selective sst_2 antagonist, D-Tyr^8-CYN154806 (Ac-(4-NO_2-Phe)-*cyc*(DCys-Tyr-DTrp-Lys-Thr-Cys)-DTyr-NH_2) (Feniuk *et al.*, 2000; Nunn *et al.*, 2003) for each recombinant sst_2 receptor was also determined and the antagonist used to confirm the predominant involvement of this receptor type in SRIF-14 responses in rat colon mucosa.

Methods

Cell culture and transfection

Colony 1 adenocarcinoma cells (from Dr S Kirkland; Marsh *et al.*, 1993) were incubated in DMEM supplemented with 10% foetal calf serum, $100\,\mu g\,ml^{-1}$ kanamycin and $1.2\,\mu g\,ml^{-1}$ amphotericin B. Cell lines were grown at 37°C in a humidified atmosphere of 95% O_2/5% CO_2 and passaged when confluent by trypsinization (0.25% in versene). Stably transfected clones were generated by calcium phosphate co-precipitation followed by glycerol shock, using cDNA sequences encoding human sst_{2a} (in pTEJ8, provided by Professor T. Schwartz, Panum Institute, Copenhagen, Denmark), and the rat sst_{2a} or sst_{2b} splice variants (N-terminal haemagglutinin (HA) epitope-tagged constructs in pcDNA3.1, from Dr M Schindler; Schindler *et al.*, 1998). Colonies resistant to the antibiotic G418 ($1.0\,mg\,ml^{-1}$) were isolated directly, expanded and screened for sst_2 receptor expression in short-circuit current (I_{SC}) studies.

Animals

Male Sprague–Dawley rats (200–250 g, from Banton and Kingman, Hull, UK) were maintained in a 12 h light–dark cycle, with access to standard chow and water *ad libitum*. The descending colon was removed from rats killed by cervical dislocation, and placed in oxygenated Kreb's Henseleit (KH) buffer (constituents in mM: NaCl 118, KCl 4.7, $NaHCO_3$ 25, KH_2PO_4 1.2, $MgSO_4$ 1.2, $CaCl_2$ 2.5, glucose 11.1; pH 7.4) until dissection.

Short-circuit current studies

Colony 1 epithelial layers were grown to confluence (area $0.2\,cm^2$) on collagen-coated Millipore filters, bathed at 37°C in oxygenated KH and voltage-clamped at 0 mV in Ussing chambers (DVC1000, WPI, Stevenage, UK) as described previously (Holliday *et al.*, 2005). The resulting I_{SC} was elevated by a maximal concentration of the secretagogue, vasoactive intestinal polypeptide (VIP) (30 nM, 20 min) before basolateral addition of sst_2 ligands. Unless otherwise stated, agonist concentration–response relationships were constructed from single peptide additions. For the determination of CYN154806 IC_{50} and pK_B values, epithelial layers were pretreated for 10 min with the antagonist before SRIF-14 application. At the end of each experiment, UK14,304 (1 μM) and piretanide (200 μM) were included as inhibitory controls.

Mucosal sheets from rat-descending colon (0.6 cm^2 area) were voltage-clamped at 0 mV in oxygenated KH, as described previously (Cox *et al*., 1988). Concentration–response curves to SRIF-14 and other analogues were constructed by cumulative peptide additions to the basolateral reservoir. Changes to I_{SC} levels were recorded continuously. Tetrodotoxin (TTX; 100 nM) was used to inhibit neuronal activity (as the submucous neuron innervation is intact in these preparations) before addition of the sst_2 antagonist, CYN154806 10 min later. For the determination of CYN154806 pA_2 value in mucosal preparations, the antagonist was added 10 min before the first agonist addition.

Phosphorylation measurements

Colony 1 clones were grown to 80% confluence in six-well plates, loaded with 50 μCi H_3PO_4 in phosphate-free KH buffer for 1 h at 37°C and treated with vehicle or 10 μM SRIF-14 for 5 min. HA-tagged sst_2 receptors were then immunoprecipitated as described previously (Holliday *et al*., 2005). Briefly, cells were dissolved (2 h at 4°C) in RIPA buffer (50 mM Tris, 100 mM NaCl, 10 mM NaF, 10 mM $Na_4P_2O_7$, 5 mM EDTA, 1.5% Nonidet P40, 0.5% sodium deoxycholate, 0.2% sodium dodecyl sulphate (SDS), 0.5 mM phenylmethylsulphonyl fluoride, 200 μM activated Na_3VO_4, 100 nM okadaic acid, 10 $\mu g\,ml^{-1}$ leupeptin and aprotinin; pH 8.0) and samples were equalized for protein content (BCA protein assay, Pierce, Cheshire, UK). Immunoprecipitations were carried out overnight at 4°C by addition of anti-HA antibody (rat clone 3f10, Roche Molecular Biochemicals, Lewes, UK) directly conjugated to agarose, and then the washed precipitates were denatured in Laemmli loading buffer (80°C, 3 min). Proteins were resolved by SDS-polyacrylamide gel electrophoresis (PAGE; 10% Tris-HCl Ready Gels; Biorad, Hemel Hempstead, UK) and the dried gels were exposed to pre-flashed Amersham Hyperfilm MP for 72 h at –70°C to detect ^{32}P labelling. To ensure equivalent receptor loading, immunoprecipitates resolved by SDS-PAGE were also transferred to polyvinyldifluoride membrane and probed overnight (18°C) with the 3f10 anti-HA antibody (100 $ng\,ml^{-1}$ in TBST (50 mM Tris, 150 mM NaCl, 0.1% Tween 20; pH 7.5) containing 1% BSA and 0.02% NaN_3). Western blots were developed using a goat anti-rat horseradish peroxidase-conjugated secondary antibody (1:5000 in TBST for 60 min; GE Biosciences, Little Chalfont, UK) and enhanced chemiluminescence detection (ECL plus; GE Biosciences).

Data analysis

Pooled data from I_{SC} studies present the maximal changes in I_{SC} as $\mu A\,cm^{-2}$, mean $\pm$ 1 standard error of the mean (s.e.m.). Agonist pEC_{50} values and antagonist pIC_{50} values were obtained by nonlinear iterative fits to the combined data using GraphPad Prism (version 3.03, GraphPad Software Inc., San Diego, CA, USA). Affinity estimates for CYN154806 were obtained from the Gaddum equation (pK_B, for epithelial layers) and Schild analysis (pA_2, for rat colon studies). Statistical comparisons of two data sets were performed by use of Student's *t*-test, while multiple comparisons were obtained by one-way analysis of variance with Dunnett's post-test.

Materials

Cell culture materials were from the following origin: DMEM and G418 sulphate (Invitrogen, Paisley, UK); foetal calf serum, kanamycin and amphotericin B (ICN Biomedicals, Oxford, UK); trypsin (Lorne Laboratories, Reading, UK). $H_3^{32}PO_4$ (10 $mCi\,ml^{-1}$) was from Amersham Biosciences (Little Chalfont, Bucks, UK). Agonists BIM23104C, BIM23190C, BIM23052, BIM23056 and BIM23268 (see Shimon *et al*., 1997 for sequences) were provided by Biomeasure Inc. (Milford, MA 01757, USA); while D-Tyr^8-CYN154806 and BIM23027 (McKeen *et al*., 1995) were kind gifts of Dr W Feniuk (Glaxo Institute of Applied Pharmacology, Cambridge, UK). Other peptides were purchased from Bachem (Merseyside, UK); all were stored as single use frozen aliquots of aqueous solution. Piretanide was obtained from Hoechst Marion Roussel (Swindon, UK), and other reagents were from Sigma-Aldrich (Poole, UK) or VWR International (Poole, UK). UK14,304 (5-bromo-*N*-(4,5-dihydro-1*H*-imidazol-2-yl)-6-quinoxalinamine) was prepared as a 10 mM solution in dimethylsulphoxide; other chemicals were made up as aqueous stock solutions.

Results

Epithelial responses to recombinant sst_2 receptors

We isolated stably transfected Colony 1 cell lines expressing the $hsst_{2a}$ (hS2a), $rsst_{2a}$ (rS2a) or $rsst_{2b}$ (rS2b). These clones exhibited higher basal resistances than non-transfected Colony 1 cells in I_{SC} studies, but in each case VIP-stimulated sustained elevations in I_{SC} with similar potencies (pEC_{50} range: 8.08–8.48, data not shown), reflecting electrogenic chloride secretion. Moreover, VIP responses in Colony 1, hS2a, rS2a and rS2b epithelial layers were all inhibited by subsequent UK14,304 activation of endogenous α_2 receptors (Figure1 and Table 1), or by blockade of basolateral $Na^+/K^+/2Cl^-$ co-transport using piretanide (Figure 1). However, in contrast to non-transfected host cells, basolateral SRIF-14 decreased VIP-stimulated I_{SC} in hS2a, rS2a and rS2b clones with equivalent potency (pEC_{50} range: 7.64–7.86) and similar levels of inhibition, that is, 29–43% of the VIP response after 100 nM SRIF-14 (Figure1 and Table 1). SRIF-14 (100 nM) also inhibited basal I_{SC} levels, by $-13.0 \pm 2.8\,\mu A\,cm^{-2}$ ($n = 4$) in rS2a cells and by $-13.0 \pm 3.8\,\mu A\,cm^{-2}$ ($n = 4$) in the rS2b epithelial clone. Apical SRIF-14 addition (100 nM) had little effect on VIP-elevated I_{SC} in rS2a ($-1.1 \pm 0.4\,\mu A\,cm^{-2}$, $n = 4$) or rS2b epithelial layers ($-3.5 \pm 0.5\,\mu A\,cm^{-2}$, $n = 3$), indicating pre-

Table 1 Electrophysiological parameters and responses to basolateral stimuli in untransfected Colony 1 cells and sst_2 receptor clones

Cells	*Basal R* ($\Omega\ cm^2$)	*Basal* I_{SC} ($\mu A\ cm^{-2}$)	*VIP 30* nM ΔI_{SC} ($\mu A\ cm^{-2}$)	*SRIF-14* pEC_{50}	*SRIF-14* 100 nM ΔI_{SC} ($\mu A\ cm^{-2}$)	*UK14,304* 1 µM ΔI_{SC} ($\mu A\ cm^{-2}$)
Colony 1	39.3±0.6 (531)	11.0±0.4 (531)	+29.5±1.2 (200)	—	0.0±0.0 (14)	−10.4±0.9 (4)
hS2a	131.2±4.1 (125)	9.9±4.9 (125)	+22.1±1.0 (103)	7.64±0.07	−9.6±1.1 (8)	−5.8±0.5 (6)
rS2a	100.1±2.5 (237)	50.6±1.7 (237)	+73.2±1.8 (189)	7.67±0.07	−22.4±2.2 (6)	−25.3±3.4 (6)
rS2b	63.4±2.8 (126)	25.2±1.1 (126)	+83.0±3.3 (105)	7.86±0.07	−24.3±4.4 (6)	−19.5±3.6 (6)

Abbreviations: SRIF-14, somatotrophin release inhibiting factor; UK14,304, 5-bromo-*N*-(4,5-dihydro-1H-imidazol-2-yl)-6-quinoxalinamine; VIP, vasoactive intestinal polypeptide.
pEC_{50} values for SRIF-14 were calculated from pooled single addition concentration–response relationships for the inhibition of 30 nM VIP-stimulated I_{SC} (n = 3–8). Values in parentheses indicate the number of observations for basal resistances (R) and I_{SC}, and for the change in I_{SC} (ΔI_{SC}) after each agonist addition at the optimal concentrations shown.

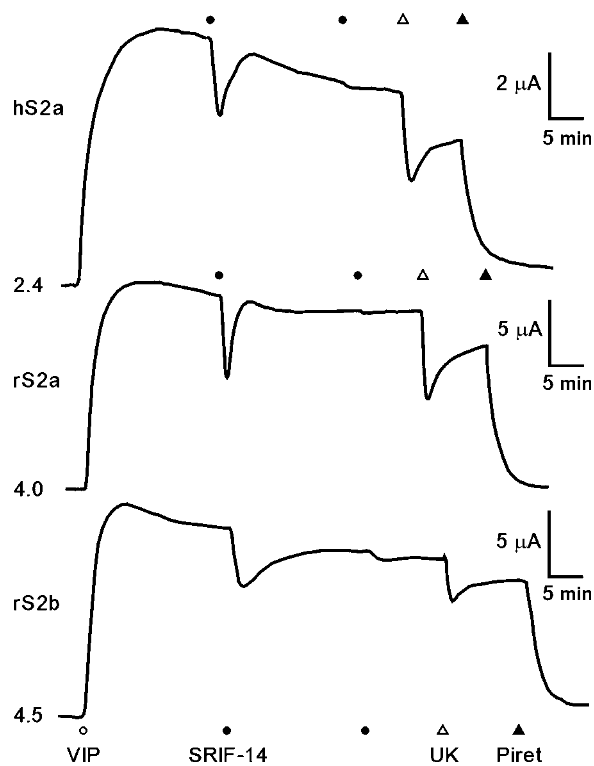

Figure 1 Representative I_{SC} recordings from Colony 1 hS2a, rS2a and rS2b clones. Confluent epithelial layers were stimulated with 30 nM vasoactive intestinal polypeptide (which produced a sustained rise in I_{SC}) then by 100 nM SRIF-14 (two additions 20 min apart), 1 µM UK14,304 (UK) and 200 µM piretanide (Piret) as indicated. Initial I_{SC} levels (in µA) are given to the left of each trace. Note the smaller µA scale for the hS2a trace. SRIF-14, somatotrophin release inhibiting factor; UK14,304, 5-bromo-*N*-(4,5-dihydro-1H-imidazol-2-yl)-6-quinoxalinamine; VIP, vasoactive intestinal polypeptide.

ferential targeting of both sst_2 receptor variants to the epithelial basolateral membrane.

Sst_{2a} and sst_{2b} receptor desensitization

Figure 2a illustrates the time-profiles of sst_{2a} and sst_{2b}-mediated I_{SC} responses following basolateral SRIF-14 addition. In both hS2a and rS2a cells, SRIF-14 responses were transient, with increased agonist concentrations leading to both a reduction in the time-to-peak (1–1.5 min after 300 nM SRIF-14), and a more rapid return to I_{SC} levels before sst_{2a} stimulation (3–4 min after 300 nM). In contrast to the short-lived nature of rat and human sst_{2a} responses, the inhibition of VIP-elevated I_{SC} by SRIF-14 in rS2b epithelial layers was more sustained (Figure 2a). For example, responses at 10 min after 300 nM SRIF-14 had decayed to 47.2±3.3% (n = 4) of the peak levels at 2.5–3 min, compared to only 6.4±1.8% (n = 5; P < 0.001) in rS2a cells.

We next compared rS2a and rS2b concentration–response curves constructed from single agonist additions, with cumulative relationships in which sequential applications of agonist were made at the peak of the previous SRIF-14 response (Figure 2b). The cumulative data for rS2b clones yielded a SRIF-14 pEC_{50} of 7.83±0.04 and a maximal I_{SC} response of −21.8±3.4 $\mu A\ cm^{-2}$ (n = 4, 144 nM), similar to values obtained from single peptide additions (Table 1). However, rS2a cumulative SRIF-14 responses were bell-shaped, with a 10-fold higher pEC_{50} for the inhibitory portion of the curve (8.55±0.08), and a maximal response at 44 nM (−7.0±0.6 $\mu A\ cm^{-2}$, n = 4) that was only 31% of the peak I_{SC} decrease to 100 nM SRIF-14 (Table 1).

To measure phosphorylation, the HA-tagged rat sst_{2a} and sst_{2b} receptors were immunoprecipitated from epithelial clones loaded with $^{32}P_i$, and incorporation of radiolabelled phosphate was determined by gel autoradiography. These experiments were technically challenging, involving the use of a high agonist concentration (10 µM SRIF-14 for 5 min) to overcome the diffusion barrier to the basolateral epithelial domain, and limited by variable background in the autoradiographs from the presence of genomic DNA contamination in the samples. Western blots probed with anti-HA revealed specific broad bands in immunoprecipitates from rS2a (58–83 kDa) and rS2b (53–83 kDa) epithelia (Figure 2c), which were absent in samples from non-transfected Colony 1 cells. Despite the similar loading of receptor proteins, $^{32}P_i$ labelling of an equivalent band was observed only in rS2a immunoprecipitates (autoradiograph, Figure 2c), following stimulation by SRIF-14. In contrast, no phosphorylation of sst_{2b} receptors could be detected.

Effects of sst agonists and antagonist CYN154806 on recombinant sst_2 receptor-expressing epithelia

The sst_2-preferred peptides BIM23027 and BIM23190C were both full agonists in the transfected clones (Figure 3), displaying equivalent potencies and response time-profiles to SRIF-14 in rS2a and rS2b epithelial layers. BIM23027

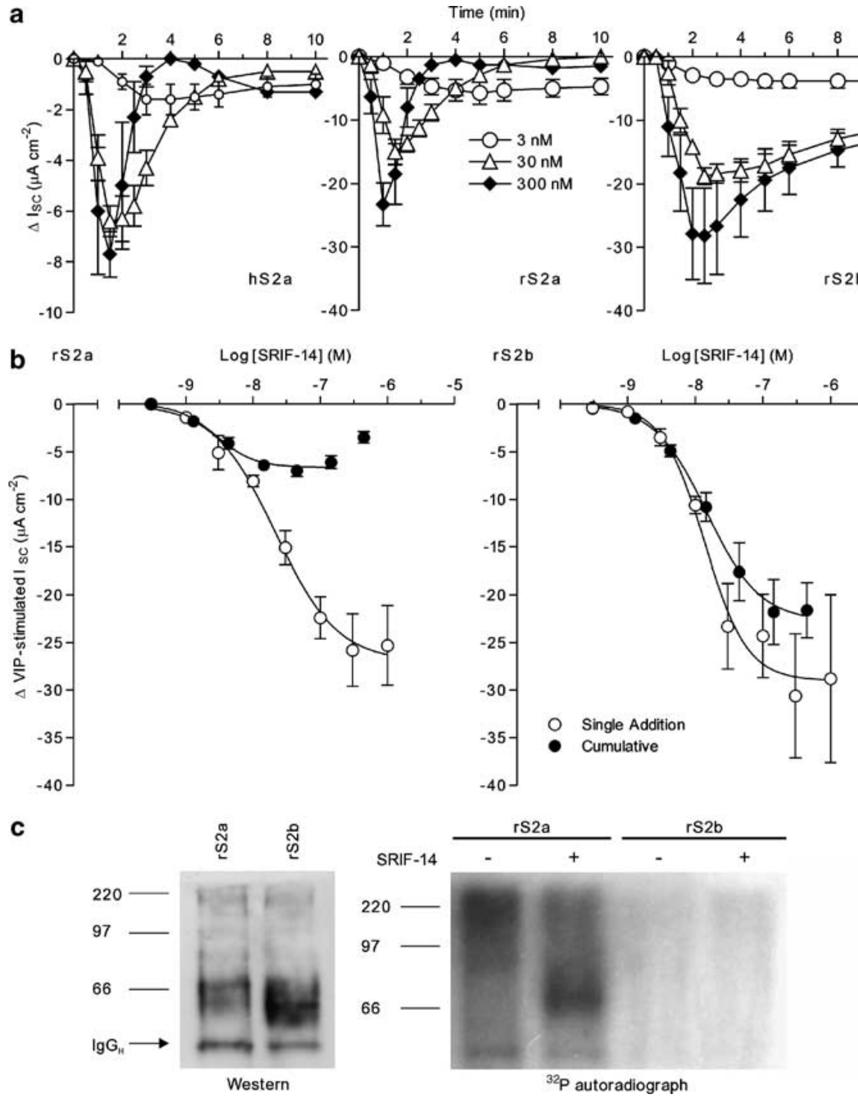

Figure 2 Desensitization of sst_{2a} and sst_{2b} receptors. Time courses from hS2a, rS2a and rS2b cells (**a**) show the reductions in vasoactive intestinal polypeptide-stimulated I_{SC} following SRIF-14 addition ($t=0$), at 3 nM ($n=3$–4), 30 nM ($n=3$–4) or 300 nM ($n=3$–5). SRIF-14 concentration–response relationships in rS2a and rS2b epithelial layers (**b**) were constructed from responses to single agonist concentrations ($n=3$–8), or to cumulative agonist additions ($n=3$–4). Sigmoidal fits to the pooled data (excluding the 444 nM data point for rS2a-cumulative responses) yielded the pEC_{50} values and maximal SRIF-14 responses given in Table 1 and the text. In (**c**), immunoprecipitated HA-tagged rat sst_{2a} and sst_{2b} receptors were resolved by SDS-PAGE and transferred to polyvinyl difluoride membrane for western blotting with anti-HA (left hand photograph). Sst_2 proteins were identified as broad bands of 58–83 kDa (sst_{2a}) and 53–83 kDa (sst_{2b}), in addition to bands corresponding to the light (25 kDa, data not shown) and heavy (IgG_H) chains of the immunoprecipitating antibody. To measure phosphorylation, HA-tagged receptors were immunoprecipitated under the same conditions, from rS2a and rS2b cells labelled with $^{32}P_i$ and treated with vehicle or 10 μM SRIF-14 for 5 min. The autoradiograph (right, 72 h) of the dried SDS-PAGE gel indicates agonist-induced phosphorylation of rat sst_{2a}, but not sst_{2b} receptors. SDS-PAGE, sodium dodecyl sulphate-polyacrylamide gel electrophoresis; SRIF, somatotrophin release inhibiting factor

inhibited VIP-stimulated I_{SC} with pEC_{50} values of 7.41 ± 0.26 (rS2a; $n=4$) and 7.50 ± 0.18 (rS2b; $n=3$–5), BIM23190C pEC_{50} values were 7.58 ± 0.14 in rS2a cells ($n=3$–5) and 7.66 ± 0.18 in the rS2b clone ($n=3$–5). The sst_5-preferred agonist BIM23268 (100 nM) elicited only small I_{SC} decreases in each clone, with slight reductions in the subsequent sensitivity to 100 nM SRIF-14 (Figure 3). BIM23056 (a partial agonist at sst_5, sst_3 and sst_2 receptors, 100 nM) did not affect VIP-elevated I_{SC}, nor did it alter the responses to SRIF-14 added 20 min later (Figure 3).

The D-Tyr^8 isomer of the peptide sst_2 antagonist CYN154806 (1 μM) produced small increases in I_{SC}, and attenuated peak SRIF-14 responses added 10 min later in hS2a, rS2a and rS2b clones (Figure 3). CYN154806 pIC_{50} values for the inhibition of 100 nM SRIF-14 responses were 7.13 ± 0.17 (hS2a) and 7.48 ± 0.04 (rS2a; both $n=3$–6). SRIF-14 concentration–response relationships were parallel-shifted to the right to the same degree in hS2a and rS2a epithelial layers by 30 nM CYN154806, with no change in the maximum (data not shown). The resulting pEC_{50} values in the presence of antagonist were 7.17 ± 0.08 (hS2a) and 7.04 ± 0.10 (rS2a; each $n=3$–8), yielding pK_B values for the $hsst_{2a}$ and $rsst_{2a}$ receptor of 7.9 and 7.8, respectively.

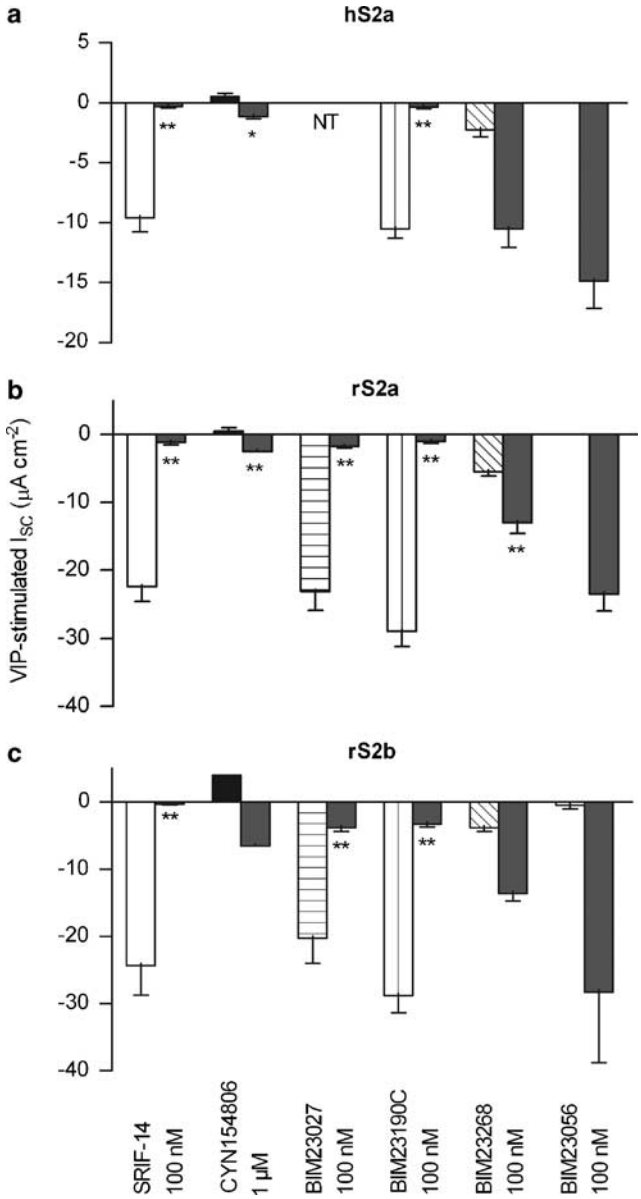

Figure 3 Responses to SRIF-14 analogues in Colony 1 clones. Epithelial layers from hS2a (**a**), rS2a (**b**) or rS2b cells (**c**) were prestimulated with 30 nM vasoactive intestinal polypeptide for 20 min, followed by SRIF-14, BIM agonists, or D-Tyr[8] CYN154806 ($n=3$–6). The pooled changes in I_{SC} to these peptides (mean$\pm$1 s.e.m.) are indicated by the left hand of each pair of columns (open for SRIF-14, filled or hatched for analogues). A second addition of 100 nM SRIF-14 was added after 20 min (SRIF-14 or BIM agonists) or 10 min (CYN154806), giving the indicated reductions in I_{SC} (right hand column of each pair). *$P<0.05$, **$P<0.01$ compared to control 100 nM SRIF-14 responses (open columns). BIM23027 was not tested (NT) in hS2a cells and CYN154806 data for rS2b was $n=1$. D-Tyr[8] CYN154806, Ac-(4-NO_2-Phe)-*cyc*(DCys-Tyr-DTrp-Lys-Thr-Cys)-DTyr-NH_2; SRIF-14, somatotrophin release inhibiting factor.

Responses to SRIF-14 and analogues in rat descending colon mucosa

Isolated preparations of rat descending colon mucosa exhibited basal resistances of $93.2\pm4.0\,\Omega\,cm^2$ and I_{SC} levels of $48.7\pm3.7\,\mu A\,cm^{-2}$ ($n=76$). SRIF-14, BIM23190C, BIM23014C, BIM23268 and BIM23052 all inhibited the basal I_{SC}, with maximal sustained responses of similar magnitude. Concentration–response relationships (Figure 4a and Table 2) revealed the following order of agonist potency: BIM23190C$\geqslant$BIM23014C$>$SRIF-14$>$BIM23052$=$BIM23268. BIM23056 was inactive up to the highest concentration tested (444.4 nM; as observed previously in colonic mucosa; McKeen *et al*., 1995) and a subsequent addition of SRIF-14 (100 nM) still reduced I_{SC} by $77.0\pm8.0\%$ ($n=6$; compared with controls of $71.2\pm5.2\%$, $n=6$).

To measure epithelial responses to these agonists in the absence of potentially confounding neuronal sst receptor-mediated effects, we added the neurotoxin, TTX (100 nM) to mucosal preparations. TTX reduced the basal I_{SC} slightly ($-5.6\pm0.9\,\mu A\,cm^{-2}$; $n=40$, as shown previously, Ferrar *et al*., 1990), but had no significant effect on the subsequent pEC_{50} values for BIM23190C (8.61 ± 0.33, $n=5$) or BIM23268 (6.84 ± 0.30, $n=4$) compared with controls (Table 2). Pre-incubation of TTX-treated tissues with CYN154806 (10 min, produced no change in I_{SC}) elicited rightward shifts in the SRIF-14 concentration–response curve without a change in the maximum inhibitory response (Figure 4b), yielding pEC_{50} values of 7.38 ± 0.01 (10 nM antagonist), 6.90 ± 0.02 (100 nM) and 6.01 ± 0.03 (1 μM, each $n=5$). The linearity and slope (0.85 ± 0.13) of the resulting Schild analysis was consistent with reversible, competitive antagonism, and gave a pA_2 value of 8.2. The BIM23190C concentration–response curve was also right-shifted (pEC_{50}: 7.20 ± 0.05, compared to 8.61 ± 0.05 in control tissues; $n=5$) in the presence of 100 nM CYN154806 and the resulting pK_B value (8.4) was similar to the pA_2 obtained with SRIF-14 as the agonist. The effect of CYN154806 on sst_5 preferred agonist, BIM23268-stimulated responses was less pronounced, with a small decrease in agonist potency after 100 nM antagonist (pEC_{50}: 7.21 ± 0.07 compared to control value of 7.49 ± 0.18, $n=3$–5), resulting in a 10-fold lower pK_B estimate of 7.0.

Discussion

SRIF-14 antisecretory responses, desensitization and phosphorylation of recombinant sst_2-expressing epithelia.

We characterized the splice variants of the human and rat sst_2 receptors in stably transfected epithelial cells, to assess how differences between their respective C termini altered functional responses. Sst_{2a} and sst_{2b} receptors were both targeted to the basolateral epithelial membrane, indicating that the shortened C-tail of the sst_{2b} receptor did not cause its apical misdirection after synthesis (Beau *et al*., 2004). In each cell line (hS2a, rS2a and rS2b), basolateral SRIF-14 inhibited VIP-stimulated I_{sc} levels (pEC_{50} 7.64–7.86), as expected from the preference of the former receptors for $G_{i/o}$ protein coupling (Schindler *et al*., 1998; Siehler and Hoyer, 1999b). However, SRIF time-courses were strikingly more transient in hS2a and rS2a cells than observed for rS2b responses. Together with the comparison between SRIF cumulative and single addition concentration–response relationships (Figure 2b), these data provide strong evidence that both sst_{2a} receptors undergo much more rapid desensitization than the $rsst_{2b}$ variant.

Table 2 The potencies and peak effect of sst receptor agonists in rat descending colon mucosa

Agonist	*Sst receptor preference and order*	*pEC₅₀*	*Peak cumulative ΔI_SC (μA cm⁻²)*
SRIF-14	Nonselective (2, 3, 5 ⩾1, 4)	7.92±0.08 (18)	−67.6±7.5 (444 nM)
BIM23190C	Sst$_2$-preferred(2≫5>3≫4, 1)	8.48±0.06 (5)	−76.7±11.9 (144 nM)
BIM23014C	Sst$_2$-preferred (2≫5>3≫4, 1)	8.21±0.05 (2–5)	−107.8±14.3 (144 nM)
BIM23052	Sst$_5$-preferred (5>3, 2⩾4⩾1)	6.46±0.03 (4)	−83.3±18.6 (4.44 μM)
BIM23268	Sst$_5$-preferred (5≫2, 4, 1>3)	6.84±0.03 (6)	−54.0±8.1 (1.44 μM)
BIM23056	Partial agonist at all (5>2, 3⩾4⩾1)	Inactive (3)	0.0±0.0 (444 nM)

Abbreviation: SRIF, somatotrophin release inhibiting factor.
The described sst receptor preferences of SRIF-14 and BIM analogues are based on binding IC_{50} values obtained at recombinant human sst_{1-5} receptors in stably transfected CHO-K1 cells (Shimon *et al.* (1997)).
pEC_{50} values (with *n* numbers) and peak agonist responses (including the highest cumulative peptide concentration used, in brackets) were calculated from the concentration–response relationships presented in Figure 4a.

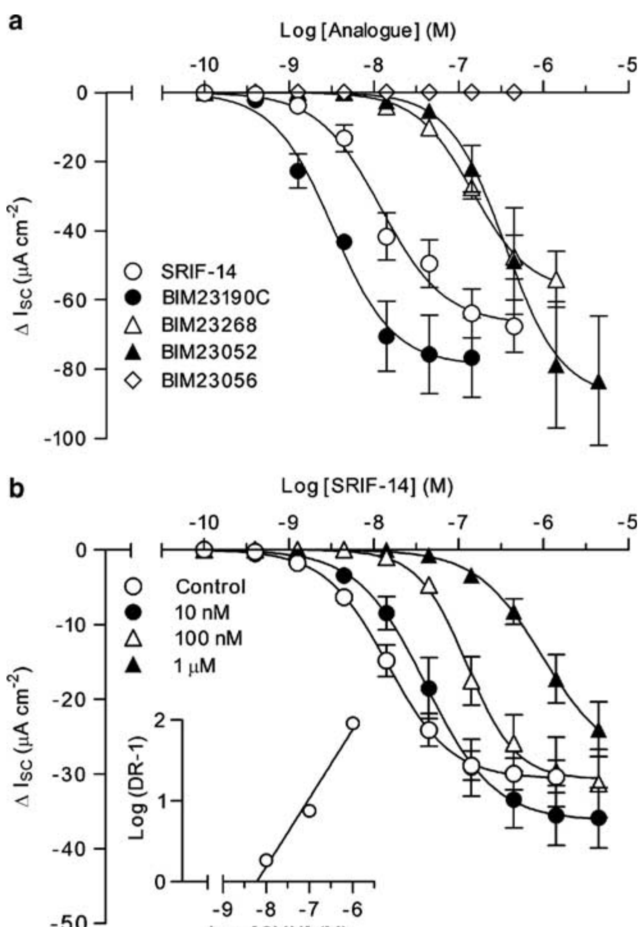

Figure 4 Responses to SRIF-14 and BIM agonists in rat descending colon mucosa. In (**a**), pooled cumulative concentration–response curves for SRIF-14 ($n=18$), BIM23190C ($n=3$–5), BIM23052 ($n=4$), BIM23268 ($n=6$) or BIM23056 ($n=3$) produced the pEC_{50} values presented in Table 2. (**b**) The effect of CYN154806 pretreatment (CYN; 10 nM–1 μM; $n=5$) on the SRIF-14 concentration–response curve (antagonist pEC_{50} values are quoted in the text) in tetrodotoxin (100 nM)-pretreated tissues. The resulting Schild plot (inset) had a slope of 0.85 and a pA_2 value of 8.2. SRIF, somatotrophin release inhibiting factor.

As we also observed in rS2a epithelial cells, native and recombinant sst_{2a} receptors are phosphorylated within minutes (Liu *et al.*, 2003, 2005; Tulipano *et al.*, 2004), either by a G-protein-coupled receptor kinase, GRK2, after homologous SRIF-14 stimulation (Elberg *et al.*, 2002; Tulipano *et al.*, 2004), or after heterologous activation of protein kinase C by other G-protein-coupled receptors (Hipkin *et al.*, 2000; Elberg *et al.*, 2002). Phosphorylated sst_{2a} receptors bound to SRIF-14 recruit β-arrestin adaptor proteins, preventing G-protein coupling (desensitization) and also initiating clathrin-mediated internalization (Tulipano *et al.* 2004). SRIF-14 and its peptide analogues (but not small molecule agonists) stimulate similar patterns of sst_{2a} β-arrestin2 recruitment and internalization (Liu *et al.*, 2005), consistent with the identical time-course profiles of SRIF-14, BIM23027 and BIM23190C in hS2a and rS2a cells. The reduced desensitization observed here for the sst_{2b} variant is supported by an earlier study on mouse sst_{2a} and sst_{2b} isoforms (Vanetti *et al.*, 1993), but differs from the comparison of rat sst_{2a} and sst_{2b} receptors made by Schindler *et al.* (1998). However, these authors used a much longer conditioning SRIF-14 treatment (60 min) to establish sst_{2a} and sst_{2b} desensitization, which contrasts with our examination of the real-time effects of a single agonist concentration over a shorter period (20 min). Our demonstration for the first time that $rsst_{2b}$ receptors (containing 3 C-terminal Ser/Thr residues) are not phosphorylated as efficiently as the $rsst_{2a}$ isoform (10 C-tail sites) suggests the underlying mechanism. In particular, alanine mutation of a C-terminal Thr cluster surrounded by acidic residues (E_{352}TTET) inhibits sst_{2a} phosphorylation and β-arrestin2 recruitment (Tulipano *et al.*, 2004), and the absence of this key sequence in the sst_{2b} receptor may be sufficient to explain its resistance to phosphorylation and functional desensitization.

Comparison of $hsst_{2a}$ and $rsst_{2a}$ receptor pharmacology and desensitization

There were no apparent differences in the sensitivity of epithelial layers expressing either $hsst_{2a}$ or $rsst_{2a}$ to SRIF-14, the sst_2 antagonist CYN154806 or BIM compounds; sst_2 agonist BIM23190C or the sst_5-preferred BIM23268. Both epithelial clones were insensitive to the nonselective sst_5/sst_2/sst_3 agonist, BIM23056. CYN154806 was a competitive antagonist, blocking antisecretory responses with the same potency (pK_B values of 7.9 and 7.8) for $hsst_{2a}$ and $rsst_{2a}$ and this was similar to the potencies obtained for the cyclic octapeptide in other functional assays (Feniuk *et al.*, 2000; they also used the D-Tyr^8 isomer of CYN154806).

The sst_5-preferred agonists, BIM23268 (Figure 3) and BIM23052 (data not shown) were partial activators at the highest concentration tested (100 nM) and they only caused partial subsequent desensitization of SRIF-14 responses. BIM23056 had no effect alone, or on subsequent SRIF-14 responses (Figure 3) and we conclude it has a very low affinity for sst_2 receptors in epithelia, or in rat mucosal preparations (see below). Our observations are in keeping with reports that BIM23056 has a higher affinity for sst_5 (Shimon *et al*., 1997; Siehler *et al*., 1998) and is actually a potent sst_5 antagonist (Wilkinson *et al*., 1996). As our epithelia only express sst_2 receptors, we would not expect to see any sst_5-mediated effects to this, or other less potent sst_5 analogues. We have ascertained that BIM23190C and BIM23037 are full sst_2 agonists, while BIM23268 and BIM23052 were less potent in all preparations. It is notable that in another colonic adenocarcinoma cell line (Col-24 cells, that constitutively express other G_i-coupled receptors; Cox *et al*., 2001) BIM23268 was a potent antisecretory agonist (exhibiting an EC_{50} value of 8.7 nM) and thus these cells appear to express sst_5 receptors constitutively (Cox *et al*., unpublished observations).

Sst_2 receptor pharmacology in rat-isolated colon mucosa

Reverse transcription-PCR analysis of crypt epithelia isolated from the rat descending colon, show expression of sst_{2a} and sst_{2b} receptors together with sst_1 transcripts and low levels of sst_5 RNA (but no sst_3 or sst_4 products, Warhurst *et al*., 1996). Given this combination of sst receptor expression, we might predict a mixed pharmacology. However, the sst_2-preferring agonists BIM23190C, BIM23014C (Table 2) and SRIF-14 were potent antisecretory agonists with similar efficacy, producing long-lasting reductions in I_{SC} (as shown previously for SRIF-14; Ferrar *et al*., 1990; McKeen *et al*., 1995). These inhibitory responses were unaffected by the neurotoxin, TTX and are therefore epithelial in origin. However, they were abolished by CYN154806, while BIM23056 (with purported $sst_5/sst_2/sst_3$ activity, Weckbecker *et al*., 2003; and sst_5 antagonism; Wilkinson *et al*., 1996) had no significant sst_2 activity in our epithelial models. Colonic SRIF-14 and BIM23190C responses were both blocked by CYN154806 (with a pA_2 value of 8.2 and pK_B of 8.4, respectively) and the cyclic octapeptide was an order of magnitude less potent at inhibiting the antisecretory responses of sst_5-preferred (but also sst_2-activating) BIM23268 (pK_B of 7.0). CYN154806 has in addition been found to have a low affinity for sst_5 receptors (two orders of magnitude less than its reported sst_2 affinity; Feniuk *et al*., 2000; Nunn *et al*., 2003), so inhibition, albeit at high nanomolar antagonist concentrations might be expected in colonic mucosa.

In conclusion, the rapid agonist-induced sst_{2a} receptor phosphorylation and coincident desensitization that we have observed is consistent with the pronounced sst_{2a} receptor internalization that Cole and Schindler (2000) and others (Hipkin *et al*., 2000) described. This acute process has already been harnessed to deliver stable radiolabelled SRIF-14 analogues into sst_2-expressing neuroendocrine tumours to allow either imaging (Breeman *et al*., 2001) or targeted chemotherapy and radiotherapy treatment (for a review, see Hofland and Lamberts, 2003; Weckbecker *et al*., 2003). However, certain patients with islet or carcinoid tumours can become insensitive to treatment with long-term SRIF-agonists such as lanreotide or octreotide (Hofland and Lamberts, 2003; Zomerhuis *et al*., 2005). It remains to be seen whether sst_{2a} receptor desensitization contributes in any way to this chronic reduction in efficacy.

Acknowledgements

This work was initially funded by the Special Trustees for St Thomas Hospital and subsequently the Kimmel Cancer Foundation. We thank Biomeasure Inc. (Milford, MA 01757, USA) for the BIM analogues, and Dr W. Feniuk (then at Glaxo Institute of Applied Pharmacology, University of Cambridge, UK) for BIM23027 and CYN154806. We also thank Professor T Schwartz (Panum Institute, Copenhagen, Denmark) and Dr M Schindler (now at Boehringer Ingelheim Pharma KG, Biberach an der Riss, Germany) for generously providing $hsst_{2a}$, $rsst_{2a}$ and $rsst_{2b}$ cDNA's respectively.

Conflict of interest

The authors state no conflict of interest.

References

Alderton F, Fan T-PD, Schindler M, Humphrey PPA (1998). Rat somatostatin $sst_{2(a)}$ and $sst_{2(b)}$ receptor isoforms mediate opposite effects on cell proliferation. *Br J Pharmacol* **125**: 1630–1633.

Allen JP, Canty AJ, Schulz S, Humphrey PPA, Emson PC, Young HM (2002). Identification of cells expressing somatostatin receptor 2 in the gastrointestinal tract of *sstr2* knockout/*lacZ* knockin mice. *J Comp Neurol* **454**: 329–340.

Alumets J, Sundler F, Håkanson R (1977). Distribution, ontogeny and ultra-structure of somatostatin-immunoreactive cells in the pancreas and the gut. *Cell Tissue Res* **185**: 465–479.

Beau I, Groyer-Picard MT, Desroches A, Condamine E, Leprince J, Tome JP *et al*. (2004). The basolateral sorting signals of the thyrotropin and luteinizing hormone receptors: an unusual family of signals sharing an unusual distal intracellular localization, but unrelated in their structures. *Mol Endocrinol* **18**: 733–746.

Breeman WA, de Jong M, Kwekkeboom DJ, Valkema R, Bakker WH, Koojj PP *et al*. (2001). Somatostatin receptor-mediated imaging and therapy: basic science, current knowledge, limitations and future perspectives. *Eur J Nucl Med* **28**: 1421–1429.

Cole SL, Schindler M (2000). Characterisation of somatostatin sst_2 receptor splice variants. *J Physiol* **94**: 217–237.

Cox HM, Cuthbert AW, Håkanson R, Wahlestedt C (1988). The effect of neuropeptide Y and peptide YY on electrogenic ion transport in rat intestinal epithelia. *J Physiol* **398**: 65–80.

Cox HM, Tough IR, Zandvliet DWJ, Holliday ND (2001). Constitutive neuropeptide Y Y_4 receptor expression in human colonic adenocarcinoma cell lines. *Br J Pharmacol* **132**: 345–353.

Ekblad E, Ekman R, Håkanson R, Sundler F (1988). Projections of peptide-containing neurons in rat colon. *Neuroscience* **27**: 655–674.

Eklund S, Sjöqvist A, Fahrenkrug J, Jodal M, Lundgren O (1988). Somatostatin and met-enkephalin inhibit cholera toxin-induced jejunal net fluid secretion and release VIP in the cat *in vivo*. *Acta Physiol Scand* **133**: 551–557.

Elberg G, Hipkin RW, Schonbrunn A (2002). Homologous and heterologous regulation of somatostatin receptor 2. *Mol Endocinol* **16**: 2502–2514.

Feniuk W, Jarvie E, Luo J, Humphrey PPA (2000). Selective somatostatin sst_2 receptor blockade with the novel cyclic octapeptide, CYN-154806. *Neuropharmacology* **39**: 1443–1450.

Ferrar JA, Cuthbert AW, Cox HM (1990). The antisecretory effects of somatostatin and analogues in rat descending colon mucosa. *Eur J Pharmacol* **184**: 295–303.

Gugger M, Waser B, Kappeler A, Schonbrunn A, Reubi JC (2004). Cellular detection of sst_{2A} receptors in human gastrointestinal tissue. *Gut* **53**: 1431–1436.

Hicks GA, Feniuk W, Humphrey PPA (1998). Outward current produced by somatostatin (SRIF) in rat anterior cingulated pyramidal cells *in vitro*. *Br J Pharmacol* **124**: 252–258.

Hipkin RW, Wang Y, Schonbrunn A (2000). Protein kinase C activation stimulates the phosphorylation and internalization of the sst2A somatostatin receptor. *J Biol Chem* **275**: 5591–5599.

Hofland LJ, Lamberts SWJ (2003). The pathophysiological consequences of somatostatin receptor internalization and resistance. *Endocrinol Rev* **24**: 28–47.

Holliday ND, Lam C-W, Tough IR, Cox HM (2005). Role of the C-terminus in neuropeptide Y Y_1 receptor desensitisation and internalisation. *Mol Pharmacol* **67**: 655–664.

Kleuss C, Hescheler J, Ewel C, Rosenthal W, Schultz G, Wittig B (1991). Assignment of G-protein subtypes to specific receptors inducing inhibition of calcium currents. *Nature* **353**: 43–48.

Knobloch SF, Diener M, Rummel W (1989). Antisecretory effects of somatostatin and vasopressin in the rat colon descendens *in vitro*. *Reg Peptides* **25**: 75–85.

Lamberts SWJ, van der Lely A, de Herder WW, Hofland LJ. (1996). Octreotide. Drug therapy. *New Engl J Med* **334**: 246–254.

Liu Q, Cescato R, Dewi DA, Rivier J, Reubi J-C, Schonbrunn A (2005). Receptor signaling and endocytosis are differentially regulated by somatostatin analogs. *Mol Pharmacol* **68**: 90–101.

Liu Q, Reubi J-C, Wang Y, Knoll BJ, Schonbrunn A (2003). *In vivo* phosphorylation of the somatostatin 2A receptor in human tumors. *J Clin Endocrinol Metabol* **88**: 6073–6079.

Lloyd KCK, Wang J, Aurang K, Gronhed P, Coy DH, Walsh JH (1995). Activation of somatostatin receptor subtype 2 inhibits acid secretion in rats. *Am J Physiol* **268**: G102–G108.

Marsh KA, Stamp GW, Kirkland SC (1993). Isolation and characterisation of multiple cell types from a single human colonic carcinoma. *J Pathol* **170**: 441–450.

McKeen ES, Feniuk W, Humphrey PPA (1995). Somatostatin receptors mediating inhibition of basal and stimulated electrogenic ion transport in rat isolated distal colonic mucosa. *Naunyn-Schmied Arch Pharmacol* **352**: 402–411.

Nunn C, Schoeffter P, Langenegger D, Hoyer D (2003). Functional characterization of the putative somatostatin sst2 receptor antagonist CYN 154806. *Naunyn-Schmied Arch Pharmacol* **367**: 1–9.

Sarret P, Botto JM, Vincent JP, Mazella J, Beaudet A (1998). Preferential expression of sst2A over sst2B somatostatin receptor splice variant in rat brain and pituitary. *Neuroendocrinology* **68**: 37–43.

Schindler M, Humphrey PPA (1999). Differential distribution of somatostatin sst2 receptor splice variants in rat gastric mucosa. *Cell Tissue Res* **297**: 163–168.

Schindler M, Kidd EJ, Carruthers AM, Wyatt MA, Jarvie EM, Sellers LA *et al*. (1998). Molecular cloning and functional characterization of a rat somatostatin $sst_{2(b)}$ receptor splice variant. *Br J Pharmacol* **125**: 209–217.

Schultzberg M, Hökfelt T, Nilsson G, Terenius L, Rehfeld JF, Brown M *et al*. (1980). Distribution of peptide- and catecholamine-containing neurons in the gastrointestinal tract of rat and guinea-pig. *Neuroscience* **5**: 689–744.

Schulz S, Handel M, Schreff M, Schmidt H, Höllt V (2000). Localisation of five somatostatin receptors in the rat central nervous system using subtype-specific antibodies. *J Physiol* **94**: 259–264.

Shimon I, Yan X, Taylor JE, Weiss MH, Culler MD, Melmed S (1997). Somatostatin receptor subtype specificity in human fetal pituitary cultures, differential role of SSTR2 and SSTR5 for growth hormone, thyroid-stimulating hormone, and prolactin regulation. *J Clin Invest* **99**: 789–798.

Siehler S, Hoyer D (1999a). Characterisation of human recombinant somatostatin receptors. 2. Modulation of GTPγS binding. *Naunyn-Schmied Arch Pharmacol* **360**: 500–509.

Siehler S, Hoyer D (1999b). Characterisation of human recombinant somatostatin receptors. 3. Modulation of adenylate cyclase activity. *Naunyn-Schmied Arch Pharmacol* **360**: 510–521.

Siehler S, Seuwen K, Hoyer D (1998). [^{125}I][Tyr^3]octreotide labels human somatostatin sst_2 and sst_5 receptors. *Eur J Pharmacol* **348**: 311–320.

Siehler S, Seuwen K, Hoyer D (1999). Characterisation of recombinant somatostatin receptors. 1. Radioligand binding studies. *Naunyn-Schmied Arch Pharmacol* **360**: 488–499.

Tulipano G, Stumm R, Pfeiffer M, Kreienkamp HJ, Höllt V, Schulz S (2004). Differential beta-arrestin trafficking and endosomal sorting of somatostatin receptor subtypes. *J Biol Chem* **279**: 21374–21382.

Vanetti M, Vogt G, Höllt V (1993). The two isoforms of the mouse somatostatin receptor (mSSTR2A and mSSTR2B) differ in coupling efficiency to adenylate cyclase and in agonist-induced receptor desensitisation. *FEBS Lett* **331**: 260–266.

Warhurst G, Higgs NB, Fakhoury H, Warhurst AC, Garde J, Coy DH (1996). Somatostatin receptor subtype 2 mediates somatostatin inhibition of ion secretion in rat distal colon. *Gastroenterology* **111**: 325–333.

Weckbecker G, Lewis I, Albert R, Schmid HA, Hoyer D, Bruns C (2003). Opportunities in somatostatin research: biological, chemical and therapeutic aspects. *Nat Rev Drug Disc* **2**: 999–1017.

Wilkinson GF, Thurlow RJ, Sellers LA, Coote JE, Feniuk W, Humphrey PPA (1996). Potent antagonism by BIM-23056 at the human recombinant somatostatin sst_5 receptor. *Br J Pharmacol* **118**: 445–447.

Zomerhuis MT, Hussain SM, Feelders RA, van der Lely AJ, de Herder WW (2005). Octreotide exerts only acute, but not sustained, effects on MRI enhancement of liver metastases in carcinoid syndrome. *Neuroendocrinology* **82**: 41–48.